Lasers in Surgery and Medicine 25:107–122 (1999)

Eyelid Resurfacing

David M. Harris, PhD,[1,2,3*] Daniel Fried, PhD,[3] Lou Reinisch, PhD,[4] Thomas Bell, MD,[5] Daniel Schachter, MD,[6] Lynn From, MD,[6] and John Burkart, PhD[7]

[1]Department of Surgery, Yale University School of Medicine, New Haven, Connecticut 06520
[2]Department of Oral Biology, University of Illinois School of Dentistry at Chicago, Chicago, Illinois 60612
[3]Biomaterials and Bioengineering, Department of Restorative Dentistry, University of California, San Francisco, California 94143
[4]Department of Otolaryngology, Vanderbilt University, Nashville, Tennessee 37252
[5]Department of Plastic Surgery, University of Toronto, Toronto, Ontario M5S 1A8, Canada
[6]Department of Dermatology, Women's College Hospital, Toronto, Ontario M5S 1B2, Canada
[7]Burkart Associates, Salt Lake City, Utah

Background and Objective: **Laser resurfacing of eyelids was examined in a series of experiments designed to measure beam parameters, surface temperatures, ablation characteristics, thermal damage, tissue responses and clinical outcomes. These data were collected for the purpose of developing a logical basis for clinical dosimetry.**
Study Design: **All experiments were conducted with similar short-pulse CO_2 lasers (TruPulse, Albuquerque, NM) where the beam had been carefully characterized and calibrated. The chronological sequence examined begins with the photophysical laser/tissue interactions during the first few μsec of irradiation and ends with an evaluation of the efficacy of wrinkle reduction nine months after treatment.**
Results: **Eyelid tissue removed by the first and second passes consisted mostly of epidermis with about 38 μm of thermal damage into the papillary dermis. Erythema resolved within four weeks and most patients experienced 70–100% wrinkle reduction by nine months.**
Conclusion: **A layer of contracted dermal scar tissue that replaced the thermally challenged zone in the dermis is identified as the substrate for wrinkle reduction. The data support the following dosimetry for periorbital wrinkle reduction: One pass 4–6 J/cm^2 (350–500 mJ into a 3 × 3 mm spot). A second treatment after 9–12 months may be more beneficial than a second pass. Lasers Surg. Med. 25:107–122, 1999.**

Key words: pulsed CO_2 laser; thermal camera; infrared radiometry; histology; ablation rate; thermal necrosis; erythema; rhytides (wrinkles)

INTRODUCTION

Improvement in facial rhytides following resurfacing with the carbon dioxide laser has been reported [1–7]. However, because many techniques and laser systems have been applied for a variety of in vitro measurements, animal studies, and clinical trials it is often difficult to compare results from one study to another. Also, different subsets of facial rhytides (e.g., forehead, periorbital, perioral, etc.) respond differently to laser resurfacing. In order to overcome these difficulties we focused our research program on eyelid wrinkles, and applied several methodologies to examine, in depth, this specific clinical application. Only one type of resurfacing laser (TruPulse,

*Correspondence to: David M. Harris, PhD, 4256 Heyer Ave., Castro Valley, CA 94546. E-mail: bmcinc@earthlink.net
Accepted 7 April 1999

Albuquerque, NM, short-pulse CO_2) was used with consistent, calibrated laser parameters across studies. This has allowed us to generalize from one study to another. Other investigators using the TruPulse Laser also participated in this research program [8–20]. Their results are summarized in this report in the Discussion.

By this strategy one can provide a detailed chronological sequence of tissue effects beginning with the photophysical events during the first few microseconds and extending out to clinical assessment of wrinkle reduction at nine months post-resurfacing. From these data we offer the clinician a logical basis for defining a range of safe and effective laser parameters that optimize eyelid wrinkle reduction and minimize unfavorable side effects such as erythema and prolonged healing.

Since several different measurement techniques and tissue models were employed and included in this report, the methods and results are partitioned into separate sections in order to avoid confusion and redundancy.

LASERS

Five CO_2 laser systems ($\lambda = 10.6$ μm) with pulse durations from 0.06–0.1 ms were used in these investigations. The first was designed as an α-test unit for human facial skin resurfacing (Pulse Systems, Inc., Los Alamos, NM) and installed at the Institute for Aesthetic Plastic Surgery, Toronto, Ontario, Canada. A second Pulse Systems Scientific Laser, at the University of California, San Francisco, was used for in vitro studies. Clinical studies were conducted in Toronto. The α-unit was used on the first seven patients. Two prototype Tru-Pulse clinical units were used on the next 12 patients, and for the final 16 treatments, a production Tru-Pulse Laser was used. All systems operated in multimode to produce rectangular, non-gaussian spots. For all lasers single pulse energy remained constant with variation in pulse width, so the peak power increased as pulse width decreased. Pulse duration was fixed at 60 μsec for the α-unit and 100 μsec (90–110 μsec) for subsequent systems.

Energy was measured initially with Gentec ED-200 Joulemeter (calibrated 6/95, NIST traceable) and subsequently with a cross-calibrated Molectron Power Meter (PM600). The same PM600 was used for all subsequent studies. Dosimetry is expressed as fluence (J/cm^2) calculated as energy to tissue/actual spot size. Cumulative fluence was determined as fluence times number of passes (clinical) or "stacked" pulses. Repetition rate was variable from 1 to 12 Hz.

BEAM CHARACTERISTICS

The laser handpiece (10.1 cm f.l., 0.78 n.a.) was held in a micro-manipulator and positioned at variable distances from a tongue blade. Laser energy to tissue was adjusted to 250 mJ with a pulse duration of 60 μsec. Burns were made in the tongue blade at a distance of 0.5 to 3.5 cm in 2.0 mm steps. Ten pulses were delivered at 2 Hz to produce a clear burn pattern. The height and width of each burn were measured with a calibrated reticule (100 μm, Edmund) and 10× loupes. Energy measurements taken before and after each irradiation varied no more than ± 5 mJ.

Spot height and width ranged from 2.0 to 3.0 mm within a distance of 0.5–3.5 cm (Fig. 1A). The beam focused at about 2.2 cm with a long beam waist (≈ 1.0 cm). The beam cross-section tended to be rectangular out of focus. Measurements were repeated twice with consistent results. Spot area, computed from height and width data, averaged about 5 mm^2 within the beam waist. Fluence for a 250 mJ pulse is estimated as 6 J/cm^2 ± 1 (Fig. 1A). The edges of the spot were clear with a distinct transition between charred and normal surface.

The distribution of energy across the 1 mm^2 spot of the UCSF laser (spot geometry, Fig. 1B) was measured with a laser beam profilometer (Spirocon, Logan, UT). Production TruPulse lasers have a larger, 9 mm^2 spot, consequently, a lower fluence of 2.7 J/cm^2 for a 250 mJ pulse. Spot geometry was also estimated from the thermal profile (Fig. 1C) imaged with an infrared imaging radiometer (thermal camera: Inframetrics, Model 700, Billerica, MA). The camera imaged wavelengths in the broad band range of 3–12 μm at a frame rate of 60 Hz. Video frames containing images with time and temperature calibrations were recorded to magnetic tape and analyzed off-line. Shown in Figure 1C is the thermal emission from the surface of human forearm skin during irradiation with an 8.1 mm^2, 420 mJ (5.2 J/cm^2), 100 μsec duration, pulse. In all laser systems the multi-mode cavity produced rectangular spots with a fairly uniform fluence across the spot. This square, flat-topped distribution of energy is called the "Mesa Mode."

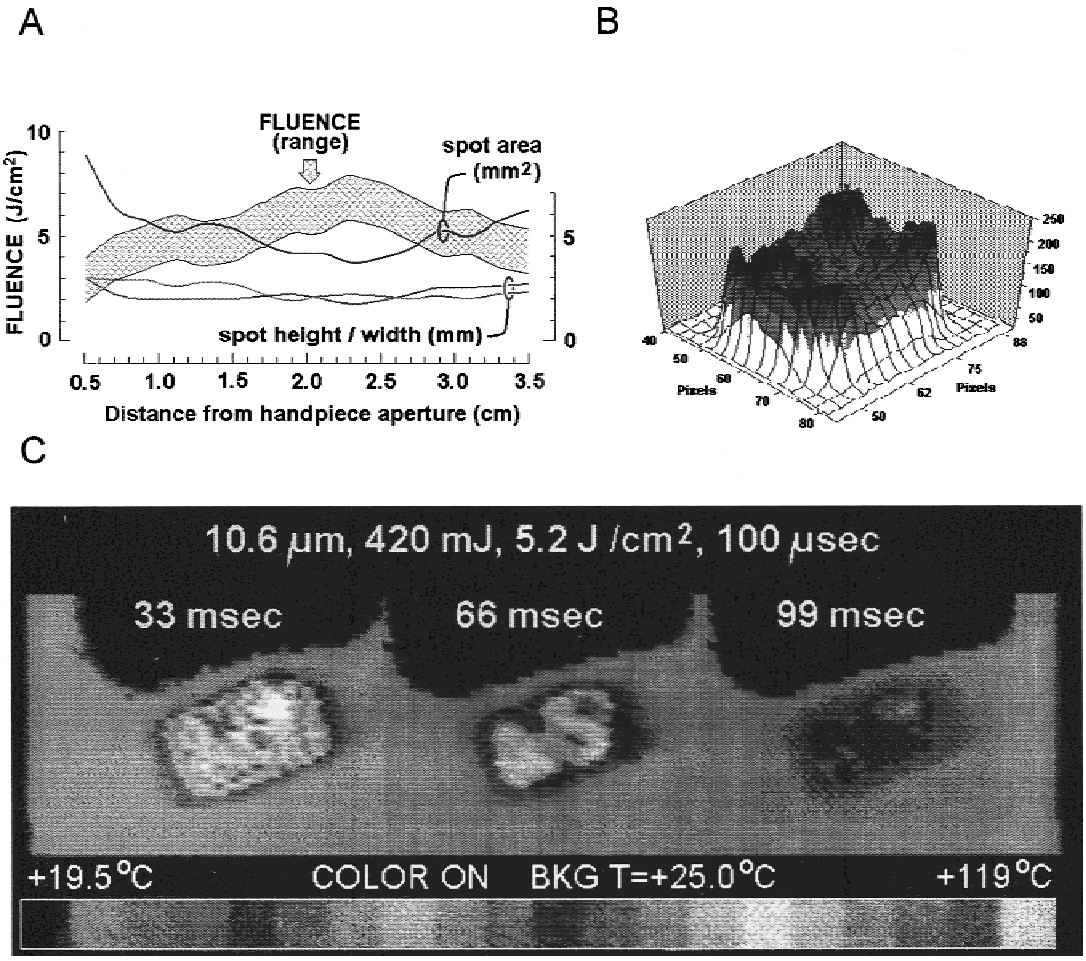

Fig. 1. The three-dimensional beam geometry of the TruPulse Laser. **A:** Longitudinal beam characteristics of TruPulse Laser #1. Fluence (J/cm^2), spot width and height (mm) and area (mm^2) are plotted as a function of distance (cm) from the handpiece aperture. **B:** Beam profile of Laser #2 (spot size: 1.0 mm^2). **C:** Three sequential frames from the thermal camera showing decay of surface temperatures on human forearm skin from a single, 100 μsec duration, 5.2 J/cm^2 impulse from Laser #3. The angle of the camera was not perpendicular to the surface (spot: 2.8 mm × 2.9 mm).

TISSUE SAMPLES

This report presents data obtained with four different target tissues. Clinical data were collected following resurfacing of lower eyelid rhytides at the Institute for Aesthetic Plastic Surgery, Toronto, Canada. Samples of redundant human upper and lower eyelid skin were obtained with permission from patients undergoing blephloplasty surgery and used to examine immediate post-treatment histology. In vivo human forearm skin was used to obtain time constants for events in the first hour post-irradiation with thermal imaging. Tissue samples used for IR radiometry were 1 cm^2 of freshly depilitated and extirpated guinea pig or mouse back full-thickness skin.

TIME-RESOLVED SURFACE TEMPERATURES

IR Radiometry of Surface Temperatures, In Vitro Skin

The tissue was kept moist until the time of irradiation when it was blotted dry with a cotton tip. The thermal emission from the tissue surface was measured during irradiation at fluences of 3–17 J/cm^2 with multiple pulses (1–20) incident upon the same area of the sample at a repetition rate of 1 Hz.

The laser beam was focused to a 1 mm^2 spot on the tissue sample surface. The sample was aligned at the first focus of a rhodium-coated, ellipsoidal reflector and the emitted thermal radiation was collected by a thermoelectrically cooled

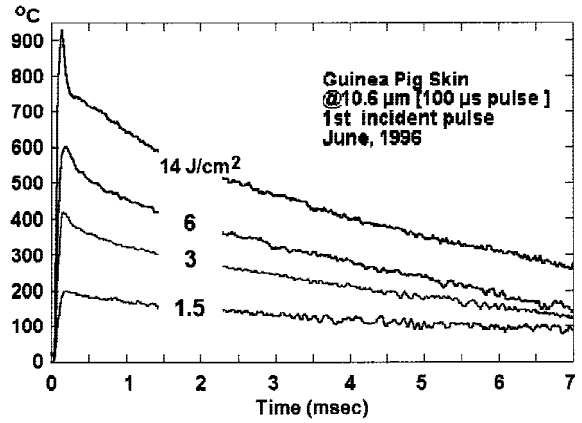

Fig. 2. Guinea pig skin temperature during CO_2 laser irradiation at l = 10.6 μm for various incident laser fluences. The pulse duration was 100 μs and each curve represents the first laser pulse on the tissue.

HgCdZnTe (HCZT) detector (BSA Technology Model PCI-L-2TE-12, Torrance, CA) placed at the second focus of the ellipse. The detector had a response time of ≈1 μs, an active area of 1 mm in diameter and collected 70% of the thermal emission above the sample (30% is lost through the entrance port of the ellipse). Two bandpass filters (Spectragon# SP-8750-F – λ = 5–9 μm) were used to limit laser radiation from reaching the detector. The detector signal was amplified, digitized, and compared with calculated values of the irradiance (W/cm^2) on the detector window to yield the surface temperature [21–24].

Figure 2 shows the radiometric temperatures measured during laser irradiation at incident fluences of 1.5, 3, 6, and 14 J/cm^2. The thermal emission from the area of the irradiated tissue increased monotonically with increasing incident laser fluence. At higher fluences there is a sharp rise in thermal emission that is present only during the duration of the laser pulse (plume component). This is particularly evident at 14 J/cm^2, but still evident at 3 J/cm^2. Surface temperature for single pulses with fluences of 4–6 J/cm^2 were in the range of 400–550°C.

In Vivo Human Forearm

Thermal emissions were imaged with an IR thermal camera following single pulses (Fig. 1C). The thermal camera temperature range provided 20 color-coded divisions. Temperature resolution was varied from 0.2 to 10°C and temporal resolution was 30 msec. Radiometric temperatures at the impact site were measured by reviewing sequential frames off-line. Single pulses ranged in energy from 100–500 mJ into an 8.1 mm^2 spot size producing fluences from 1.2–6.2 J/cm^2.

For all energies tested the surface temperatures exceeded 200°C within the first 30 msec and rapidly fell to within 5°C of baseline within 100–700 msec. There was a trend for higher energy pulses to produce higher temperatures (Fig. 3A). Post-irradiation cooling was observed with single pulses (Fig. 3B). Within the first 1–2 seconds surface temperature dropped about 2°C below pre-irradiation baseline.

Clinical Procedure

A thermal camera was used to measure the surface temperature of human eyelids in vivo during irradiation with 400 mJ laser pulses at a fluence of 4.1 J/cm^2 and a repetition rate of 8 Hz. The treatment sites were monitored with the thermal camera set to discriminate within a temperature range of 25–35°C (0.5°C resolution) over a 3 day interval. We selected this range to observe post-treatment recovery processes such as inflammation.

Pre-Tx skin temperature at the treatment site was 32.0°C (left lower lid) and 32.5°C (right lower lid). Upper eyelids and temples had +35°C hot spots. Typically, the impact site temperature stayed above 35°C for several seconds. Within a tight pattern of spots at a repetition rate of 8 Hz a specific area may stay above this value for as long as 15 seconds.

Thermal overlap and subsequent accumulation of thermal energy from adjacent impacts were clearly visible from the IR video (Fig. 4). Thus, there was a shorter time course of temperature decay with single pulses than observed clinically where sequential, adjacent pulses were delivered at a rate of 8 Hz.

We expected to see an increase in treatment site temperature immediately after the procedure, but were surprised to observe cooling (Fig. 3B). The tissue continued to cool post-irradiation to below ambient within 3–5 seconds and reached a minimum of 26.5°C (right eyelid) and 27.5 (left) within 20–30 seconds. This is –6°C (right) and –4.5°C (left). After debridement of the treatment site with saline soaked gauze the area of cooler temperatures expanded to surrounding non-treated tissues.

Cooler surface temperatures at the treatment site persisted for days. A sharp thermal gradient precisely defined the treated area. At both 21 and 70 hours a temperature differential of about 1.5°C still existed (Fig. 4, inset).

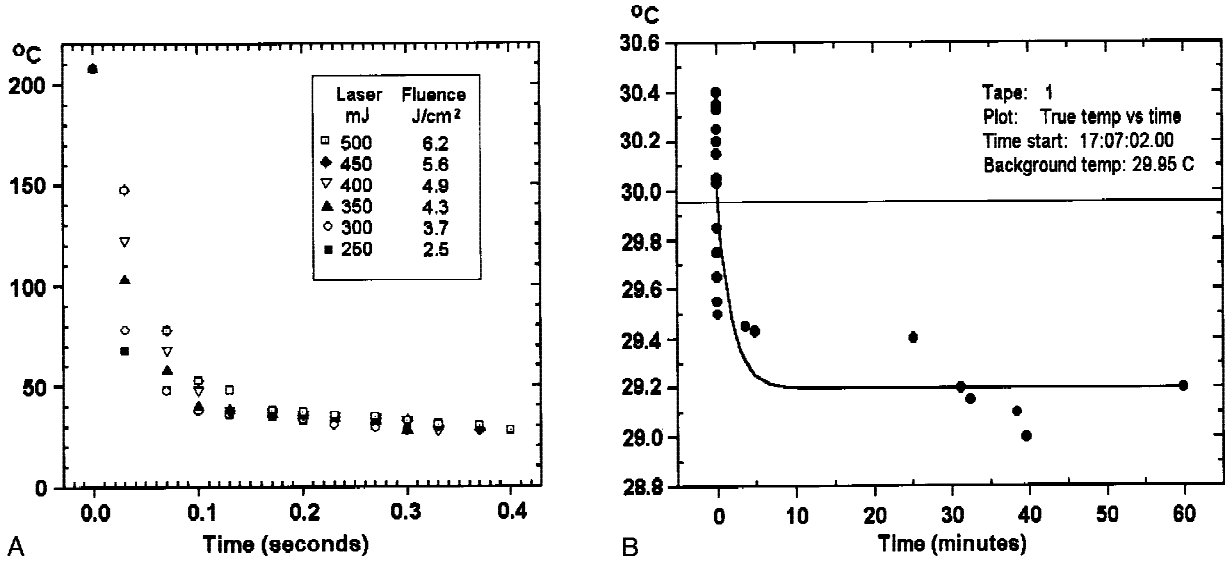

Fig. 3. **A:** Thermal relaxation of human forearm skin following single pulses. **B:** Post-irradiation cooling following a single 4.1 J/cm^2 pulse. Pre-irradiation temperature was 29.95°C.

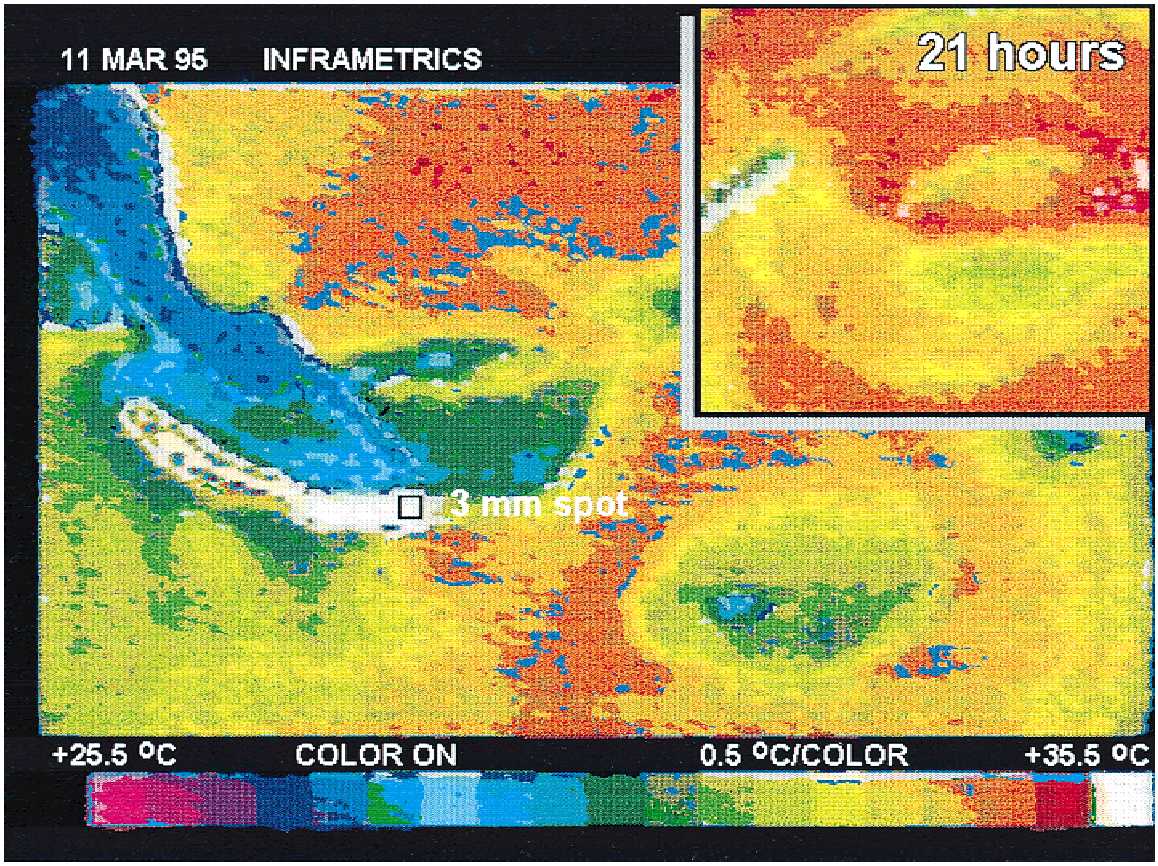

Fig. 4. Thermal camera images of the second pass during a lower eyelid resurfacing procedure. Note the area treated in the first pass is cooler and the thermal "tail" when adjacent pulses are delivered at 8 Hz. The inset shows a –2°C cooling at the treatment site 21 hours post-Tx.

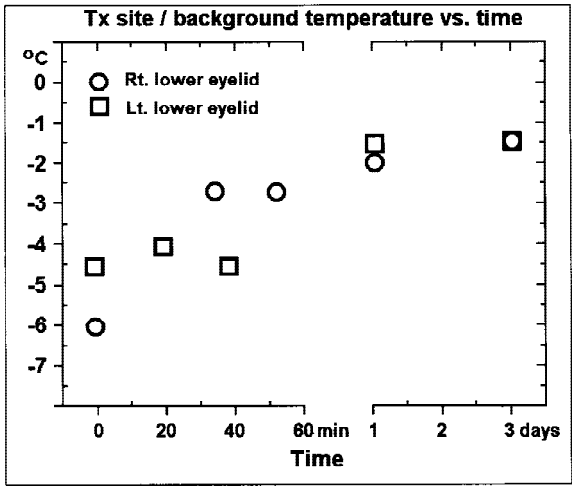

Fig. 5. Post-resurfacing cooling at the treatment site. Values are temperature differences between treatment site and surround as a function of time since treatment.

TISSUE RESPONSES

Histologic Estimates of Tissue Ablation Using In Vivo and Ex Vivo Human Eyelid Skin

The handpiece of laser #1 was held at approximately 2.0 cm from the specimen surface. Upper eyelids were irradiated in vivo with debridement between pulses. The laser pulse duration was set to 60 μsec and a single pulse energy of 250 mJ was selected to produce a fluence of 6 J/cm^2. Lower eyelids were removed and immediately irradiated ex vivo without debridement between pulses. From 4 to 7 impact sites were delivered to each tissue specimen. Sites were irradiated with 1, 2, 3, or 4 pulses (12 specimens, 55 sites). Since the handpiece was handheld, successive pulses were not always exactly in register.

Samples were pinned to dental wax, fixed in 10% formalin, sectioned, and stained with hemotoxylin and eosin (H & E). Impact sites were evaluated microscopically for depth of thermal damage, extent of lateral damage, and depth and pattern of surface ablation. Evaluation of thermal damage was based on measurements of distinct boundaries in H & E staining density using the criteria described previously by others [25–28].

Normal eyelid skin has a 5–10 μm surface layer of dead epithelial cells (stratum cornium). Below this is a uniform 30–100 μm (≈50 μm) layer of squamous epithelium. The epidermis appears thicker where skin appendages are in contact with the surface. There is a clear boundary separating epidermis from dermis (basement membrane). The epidermal/dermal interface is flat (not pappillated), and conforms to the surface topography.

No noticable plume was produced at impact with a fluence of 4.1 J/cm^2 although a white, powdery "tissue dust" was observed on the end of the handpiece and surrounding tissue. Immediately after irradiation and before debridement the skin surface appeared white at the impact site.

Histological sections through the laser impact site often showed a uniform removal of the surface layers of stratum corneum and epidermis throughout the entire spot area (Fig. 6). In samples where the spot did not move between pulses (e.g., single pulse) the crater had a distinct edge with normal tissue appearing beyond the lateral margin. Usually, islands of thermally altered epidermis remained on the surface. This was often identified as sweat duct or hair follicle epithelial tissue. These islands were seen even after four pulses. Occasionally, small vacuoles (10–30 μm) appeared in rows at the basement membrane. At irradiation sites a surface layer of dark staining, loose debris was often present (Zone 1). Crater floors were lined with 10–30 μm thick layer of dark staining necrotic tissue. Below this was a zone of increased staining, often with an amorphous, coagulated appearance (Zone 3).

Analysis of 35 impact sites indicated the Mesa Mode beam profile provided a consistent and uniform removal of tissue across the entire spot. The first 6 J/cm^2 pulse removed about 30–50 μm of epidermis and two pulses remove tissue into the papillary dermis (30–80 μm).

The extent of thermal damage was measured (Zone 2 plus Zone 3) at impact sites receiving 1–4 pulses without debridement. The depth of damage varied across any single impact site. The values used were an estimate of the average depth of damage. The average depth (± s.d.) was 38.3 (24.2) for one pulse, 45.6 (21.9) for two pulses, 28.0 (13.3) for three pulses and 40.3 (25.9) for four pulses (Table 1). The overall average was 38 μm ± 22.7 with a range of 0–100 μm. There was no detectable difference in mean depth of thermal damage as a function of number of pulses (ANOVA, $P = 0.441$). That is, with our methodology we could not determine if craters produced by four pulses were deeper than those produced by 1 pulse.

Depth of Ablation: Mouse Skin

Ablation craters were made ex vivo in mouse skin with a 1 mm square spot at energy densities of 3, 6, and 12 J/cm^2. One, two, five, 10, or 20 pulses were delivered at a rate of 1 Hz without

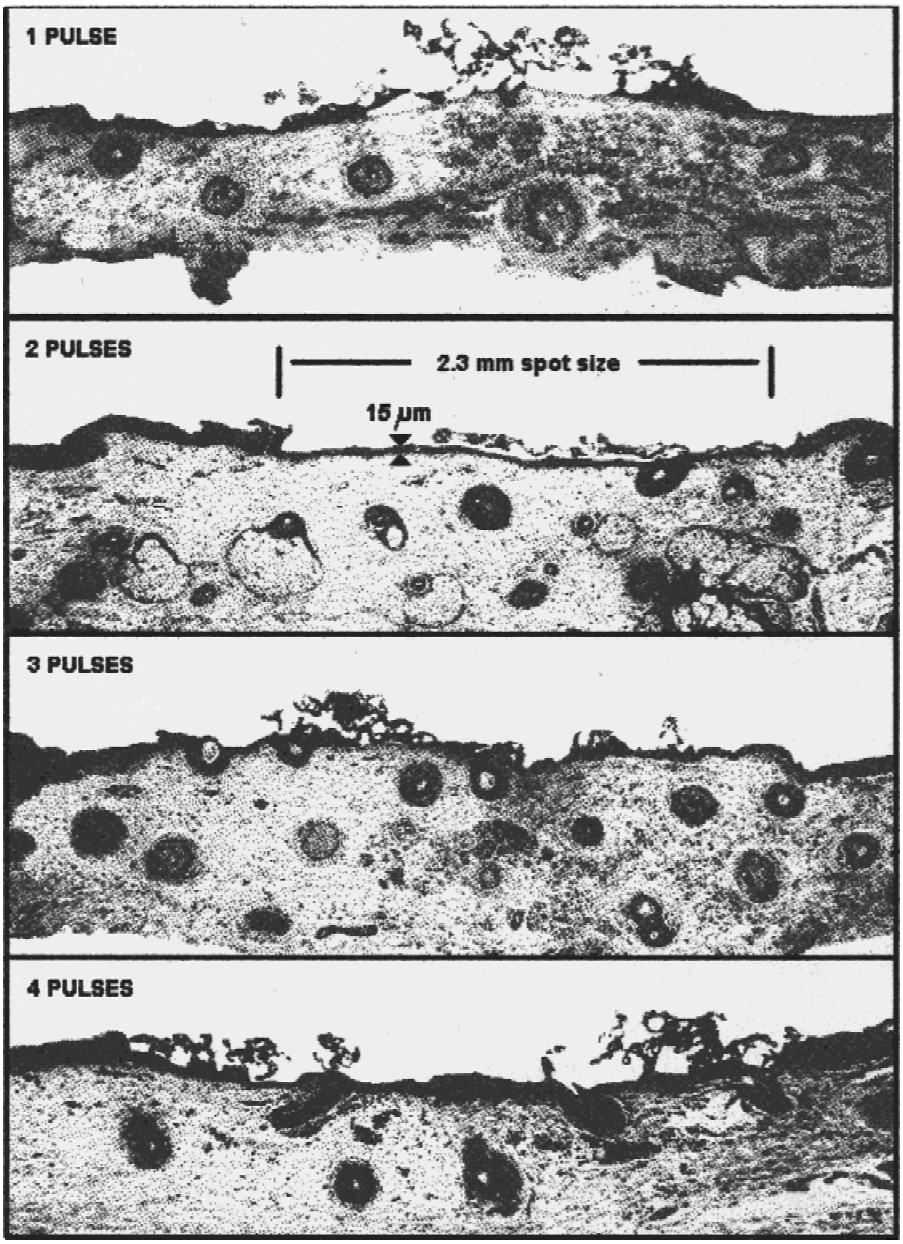

Fig. 6. Haemotoxylin and Eosin stained sections of human eyelid through four irradiation sites. Distance scale on the right is in mm. Original magnification ×40. The examples were selected from N = 55 to show the least overall thermal damage observed (average 15 μm, 2 pulses) and a worst case (average 70 μm, four pulses).

debridement between pulses. The depths of ablation craters were measured optically immediately following irradiation. The samples were examined with an optical microscope (Olympus B× 50) and Bioquant/TCW image analysis system at up to 500× magnification. The depth of ablation was measured by scanning the image plane of the microscope from the tissue sample surface surrounding the crater down to the crater floor. The vertical axis of the microscope stage was calibrated with 1 μm accuracy.

TABLE 1. Depth of Thermal Damage in Human Eyelids: 8.1 mm^2 spot, 6 J/cm^2*

	1 Pulse	2 Pulses	3 Pulses	4 Pulses
Average depth (μm)	38.3	45.6	28.0	40.3
STD	24.2	21.9	13.3	25.9

*Differences in depth of thermal damage for different number of pulses was not significant (P = 0.441).

TABLE 2. Depth of Ablation in *in Vitro* Mouse Skin: 100 μsec Duration, 1 mm² spot

	12 J/cm²		6 J/cm²	
# Pulses	Crater depth (μm)	μm/Pulse	Crater depth	μm/Pulse
20	710.9	35.5	191.7	9.6
10	306.2	30.6	93.2	9.3
5	183.7	36.7	58.6	11.7
2	61.2	30.6	−74.6	−37.3
1	39.1	39.1	0.0	0.0

Table 2 shows combined results from two sets of data. Fluences of 3 J/cm² produced no obvious surface defects. The first and second pulses sometimes resulted in raising the surface (negative depth). At higher irradiances the depth per pulse was consistent from 5–20 pulses. An increase in fluence from 6 J/cm² to 12 J/cm² resulted in an increase in ablation rate from about 10 μm/pulse to about 35 μm/pulse. The crater depth per pulse vs. the fluence for five, 10, and 20 pulses can be fit with a straight line ($R^2 = 0.986$). This model indicates a threshold of 3.1 ± 0.4 J/cm² for the ablation of tissue and 3.8 ± 0.2 μm/J/cm² of tissue removed for fluences above 3.1 J/cm².

CLINICAL PROTOCOL: LOWER EYELIDS, ERYTHEMA, AND WRINKLE REDUCTION

Patients

Patients presenting with the complaint of lower eyelid wrinkles were examined preoperatively. A history was taken with consideration of the following contraindications:

Healing disorders such as caused by diabetes or radiation/chemotherapy,
Active herpetic infection,
Allergies to topical anesthetics, antibiotics, or other medications,
Use of Accutane within last 12 months prior to resurfacing,
History of pigmentary problems (e.g., melasma, vitiligo, pigmentation following skin trauma), hypertrophic or keloid scarring,
Patients with psychiatric disorders, including alcohol or drug abuse,
Patients with unrealistic expectations,
Patients unable or unwilling to follow prescription for postoperative care.

For this study additional exclusion criteria included:

Fitzpatrick Skin Types 5 or 6,
Failure of "lid snap" test (poor tone in lower lids).

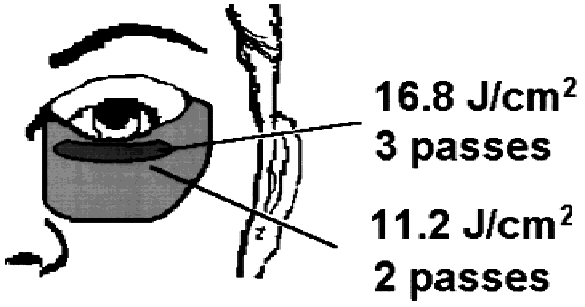

Fig. 7. Patient #9: Illustration of how dosimetry was recorded.

Treatment

Patients received Neuroleptic i.v. sedation and infraorbital nerve block and field block with 1% xylocaine with epinephrine 1:100,000. All treatments were performed by a single surgeon (TB) at the Toronto Institute for Aesthetic Plastic Surgery. Laser energy per pulse settings varied from 250 to 500 mJ (median = 400 mJ). Sequential adjacent (non-overlapping), square spots (pulses) were delivered at a repetition rate of 8 Hz in a pattern that followed lower eyelid contours. Following a complete pass the surface was debrided with sterile saline soaked gauze pads and the treatment site was examined for remaining rhytides. The number of passes ranged from 2 to 4 (median = 3) and the cumulative fluence ranged from 5 to 20 J/cm². Additional passes often did not cover the entire area treated in the first pass (Fig. 7). The treatment endpoint was the removal of all rhytides in the treatment area with noticeable tightening of the treated skin.

Postoperative care

Postoperative instructions included frequent washing (Q2–4h) with 5% acetic acid solution followed by application of a film of petrolatum. Occlusive dressings were not used. This was continued until the treated area was re-epithelized (3–5 days). Follow-up examinations and photography were scheduled for three days, one week, one, three, six, and nine months post-treatment.

Photography

Since clinical evaluations were based on viewing 35 mm patient slides, a specific effort was made to hold all photographic parameters constant. Pictures were taken (same photographer, TB) in a photographic studio with a Contax camera body with Zeiss 60 mm lens using dual Bo-

wens Monobronze DX flash with Chimera diffusers. Distance to the subject and camera settings were constant. Kodachrome 64, f8 film was obtained in a brick of 32 rolls and all images processed at the same processing lab. All make-up was removed from the treatment site prior to photography.

Quantification of Erythema

The presence or absence of erythema was determined by two evaluators who viewed patient slides. The slides were coded and examined in a random order so that evaluators did not know the time relative to treatment. "No erythema" was recorded if it was difficult for evaluators to determine if erythema was present or absent. Data were compiled as percent of patients with erythema at specific post-treatment times.

Quantification of Rhytides

Three evaluators categorized wrinkles by examination of close-up photographs of lower eyelids. Static, lower eyelid wrinkles were graded pre-treatment as mild, moderate, or severe. Typical examples for each category are shown in Figure 8. Evaluators were instructed to assign a percentage value to their judgment of wrinkle reduction. Pre-treatment and post-treatment (three months or greater) images were examined side-by-side and each evaluator made an independent estimate of percent wrinkle reduction. A value from 0–100%, derived from forced consensus, was recorded.

Data analysis

Erythema and wrinkle reduction are summarized and represented as frequency distributions. Demographic variables were age, skin type (T1–T4), and wrinkle grade (mild, moderate, severe). Treatment variables were laser number and cumulative fluence. Evaluation factors were the number of elapsed months from treatment.

Regression analysis was used to evaluate the relationships between percent wrinkle reduction and the treatment, demographic, and evaluation variables. Stepwise regression was used to search for combinations of variables influencing the percent wrinkle reduction. Scatter plots overlaid by the determined regression lines are used to visualize the relationships.

Clinical Results

From June, 1995 through June, 1996, 33 female patients received a total of 35 laser treatments for lower eyelid wrinkles. Two patients received a second treatment after the follow-up evaluation for the first treatment and are included in the analysis, for a total of 35 treatments. The average age for all treatments was 51 years. The distribution of patients into Fitzpatrick Skin Type categories was Type 1 ($N = 1$), Type 2 ($N = 14$), Type 3 ($N = 17$), and Type 4 ($N = 2$). Wrinkle grade was mild for seven treatments, moderate for 20, and severe for eight.

There was no significant bleeding nor a "chamois appearance," other common endpoints suggested in laser resurfacing [4–6]. Laser impact induced a small amount of tissue contraction. Our intra-operative endpoint was wrinkle disappearance.

Duration of Erythema

Erythema at the treatment site was visible immediately following debridement. There was usually weeping, and occasional crusting at the treatment site for 2–7 days (Average: four days). In our sample erythema resolved rapidly (Figure 9: ●). By two weeks post-treatment 50% of the patients showed no redness. At four weeks post-Tx 80% had recovered. At eight weeks one patient still had erythema that resolved by the next follow-up visit (three months). Included in the graph are data from Ostad and Moy, 1996 [29], who used a TruPulse Laser for facial scar revision (Figure 9: ■).

Percent Wrinkle Reduction

Overall the treatments were successful (Fig. 10). For 24 treatments (65%) wrinkles were rated as reduced by 70% or greater. Four patients (12%) were graded as 100% reduction—no visible wrinkles. Two patients received no reduction from the treatment. One of the latter had had blepharoplasty surgery six months prior.

When all variables were evaluated individually with respect to their relationships with percent wrinkle reduction, only month of evaluation was significant ($P = 0.033$). That is, longer evaluation times were associated with more reduction. Stepwise regression was used to determine if any other variables in addition to month were significant predictors, however, in our limited sample size none were found. The table of partial correlation coefficients shows the next most highly related variable to be the age of the patient, but its effect was not statistically significant ($P = 0.154$). Older patients tended to do better.

Skin type, wrinkle grade, laser number, and

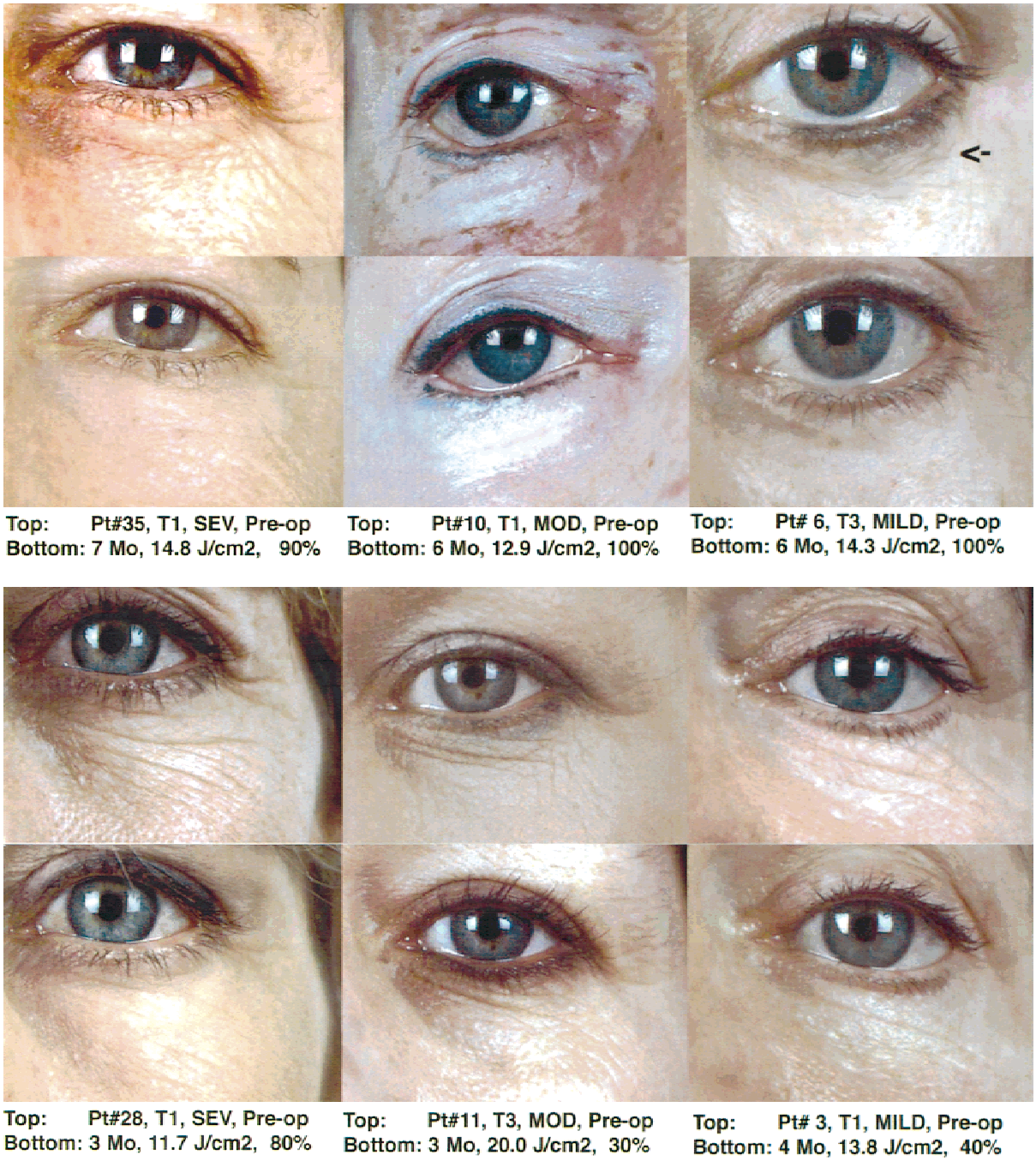

Fig. 8. Examples of wrinkle grading system (MILD, MODERATE, SEVERE) and estimates of wrinkle reduction. Dosimetry was recorded by laser settings (e.g., 450 mJ) times number of passes divided by the standard spot size of 9 mm^2 to yield total energy density in J/cm^2. A calibration factor was applied for each laser used that incorporated actual spot size and measured energy to tissue.

the cumulative fluence showed no relationship to wrinkle reduction, either with or without considering the effect of month of evaluation. Simple linear regression analyses between month and percent reduction, age and percent reduction, and cumulative fluence and percent reduction are given in Table 3. The prediction equations for these variables were:

$$\text{Percent Reduction} = 37.7 + 5.230 * \text{Month}$$
$$\text{Percent Reduction} = 32.2 + 0.653 * \text{Age}$$
$$\text{Percent Reduction} = 67.6 - 0.174 * \text{Cumulative Fluence}$$

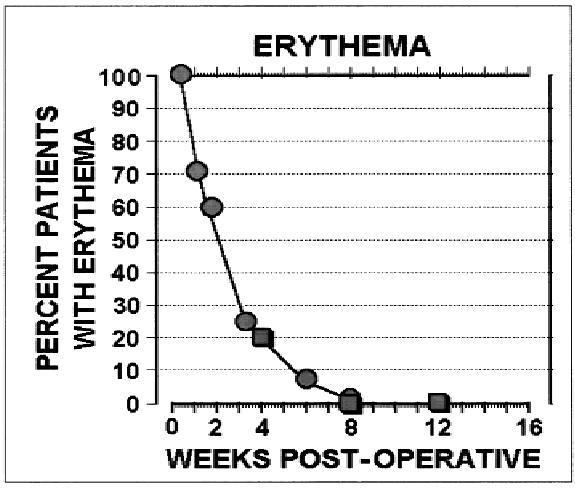

Fig. 9. Time course of recovery from erythema shown as the percent of patients with erythema as a function of evaluation time. This study ●, Ostad and Moy [29]: scar revision ■.

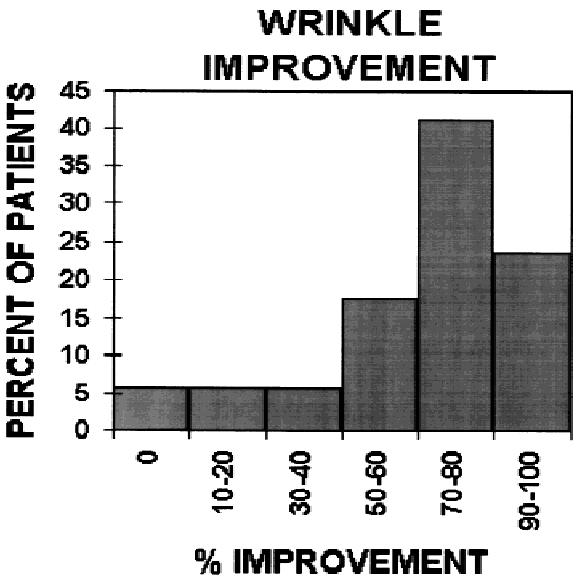

Fig. 10. Efficacy of lower eyelid resurfacing is shown as the distribution of judgments of percent wrinkle reduction within a 3–6-month post-treatment interval.

In conclusion, elapsed time from treatment was the only variable associated with outcome of percent wrinkle reduction (Fig. 11). Age of the patient showed a non-significant trend, whereas the cumulative fluence delivered had no measurable effect.

Complications

One case of transient scleral show occurred in a patient with 95% wrinkle reduction who had blethloplasty surgery six years previously. This resolved completely between 4–6 weeks. Two cases of sterile conjunctivitis were recorded, possibly related to irritation from the petrolatum.

TABLE 3. Results of the Regression Analysis

Variable	Correlation coefficient	*P*-value
Month	0.361	*0.033
Age	0.230	0.183
Cumulative fluence	–0.020	0.911
Skin type	–0.039	0.822
Wrinkle grade	0.049	0.780

*Significant at $\alpha = 0.05$.

DISCUSSION

Beam Characteristics

The TruPulse Mesa Mode provides an even fluence across the spot that results in an evenly distributed tissue effect (beam geometry = crater geometry). The square spot allows the operator to cover the treatment site with adjacent non-overlapping spots. This minimizes the accumulation of thermal energy caused by overlapping of circular spots.

Although the average fluence of a gaussian and a multimode spot can be the same, the gaussian fluence varies from 0.3 times the average at the edge ($1/e^2$ point) to 2.0 times the average at the center. The center "hot spot" in a gaussian beam may result in an overestimate of the amount of thermal damage for a given *average* fluence. Gaussian beams make gaussian-shaped craters ([8], see ref. [25, Fig. 1]).

Plume Incandescence

We identify the initial high peak temperatures measured during the laser pulse as plume incandescence. Particles in the plume can be heated to extremely high temperatures (1000's of degrees) since they are thermally isolated from the surface and can absorb the incoming laser beam energy. The emission of these particles closely follows the temporal profile of the incident laser pulse. It is most likely that the calculated temperatures are representative of the tissue surface at times greater than 1 msec after the plume emission has subsided [12].

Surface Temperatures

Choi et al. [10] measured a surface temperature of 240°C in vivo for a 3.9 J/cm^2 pulse. This is much lower than over 400°C at 4 J/cm^2 that we observed radiometrically for rodent skin in vitro. Measurements from live skin include cooling from an intact blood supply and Choi et al. [10], also

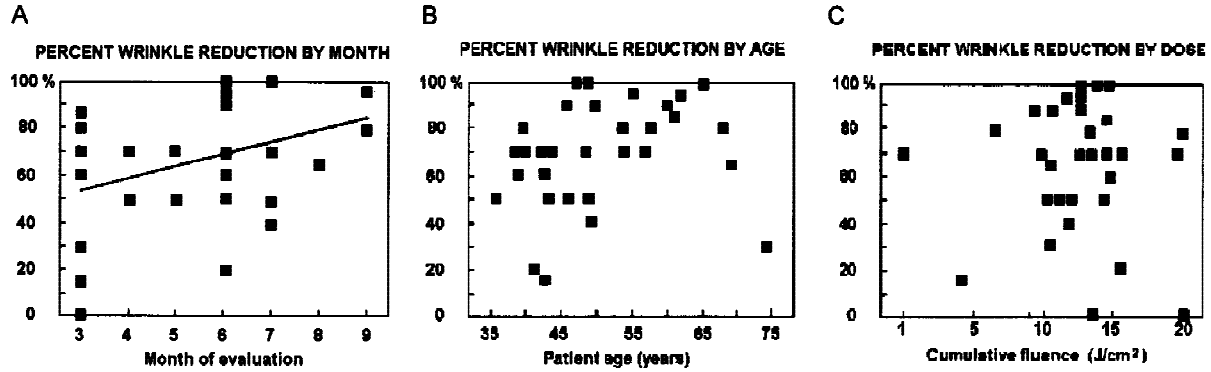

Fig. 11. **A–C**: Scatter plots of percent wrinkle reduction by month, age, and fluence. A: The line represents the best fit linear regression.

used an air stream to cool the surface and minimize thermal contributions from the plume component. Both sets of measurements indicate that temperatures well over 100°C are associated with laser ablation.

Our IR measurements were of surface temperatures. The temperatures slightly below the surface may be somewhat higher. Choi et al. [10] theorize that high rates of heat generation superheat sub-surface water, increase sub-surface pressure and, when this pressure exceeds the tensile strength of the tissue an explosive event occurs. The epidermal/dermal boundry (basal membrane) represents a transition from mainly intracellular fluids to extracellular fluids. Since energy is reflected at an interface between dissimilar media, we would predict a temperature maximum in this location.

Ablation of Epithelium

Ablation rate data for irradiation of mouse back skin and human eyelids both at 6/J/cm^2 appear to be contradictory. In the mouse, the first and second pulses sometimes resulted in raising the surface (negative depth) and the third through fifth pulses ablated about 40 μm/pulse. In the human, the first pulse ablated about 38 μm and subsequent pulses appeared to have little further effect. However, the methods for measurement varied greatly. Mouse skin was hydrated and evaluated immediate pot-irradiation in situ. Human eyelids were extirpated, dehydrated, sectioned, and stained. Furthermore, differences in morphology between mouse back skin and human eyelid skin could affect ablation depths.

Our eyelid histology showed that the first pass almost completely removes the epidermis. As mentioned above the basal membrane represents a preferential site for explosive vaporization partially separating the epidermis from the underlying dermis. Vacuoles observed in eyelid histology at this boundary and in superficial dermis in rodent skin [17,18] support this possibility. Klein et al. [30] have identified the lamina lucida as a mechanical *locus minoris resistentiae* (see also Reid [31] for a discussion of CO_2 laser surgical planes). In mouse and porcine skin the epidermis is incompletely removed [10,18]. However, recall that human eyelid upper dermis is non-papillated and thus, the epidermis may separate more readily.

Debridement between passes may affect depth of thermal damage or ablation depth. In the various experiment paradigms debridement was done when practical, however, this parameter of resurfacing was not studied systematically.

Acute Tissue Shrinkage

The acute shrinkage observed clinically after TruPulse resurfacing has been measured on human skin in vitro and porcine skin in vivo [11,15,19]. Above a threshold of 2.5 J/cm^2 the amount of shrinkage increases with each pass up to five passes to reach a maximum fractional distance decrease of about 3.6%. The contraction affects both longitudinal and radial (skin thickness) dimensions [11]. Some contraction is due to dehydration since the effect is slightly reversed when tissue is rehydrated between passes [11].

Acute shrinkage may be associated with thermal-induced changes in the extracellular protein matrix including, collagen, elastin, and hyaluronic acid. It is possible that acute shrinkage persists to provide a contracted scaffolding for long term tissue remodeling.

Immediate Histological Changes

Resurfacing initially produces lethal thermal damage to the epidermis and upper dermal

layers. Thermally altered tissues are desiccated, vacuolated, and fragmented, with thermal coagulation of proteins. We measured the depth of damage in eyelids immediately after one to three passes at 6 J/cm^2 with the TruPulse Laser to be 38 μm. This is within the range of 10–50 μm as measured by others [17–19,32].

Inflammation, Edema, and Erythema Onset

Erythema and edema of eyelid tissues increased rapidly post-treatment and was maximum within 24 hours. Speyer et al. [16] were unable to demonstrate histologically any obvious vascular changes in pig skin correlated with the time course of erythema.

Thomsen et al. [18] have described the sequence of secondary responses to TruPulse irradiation in fuzzy rat skin. In response to injury an inflammatory layer forms at the level of the intact blood supply immediately below the zone of thermal damage. Mobile recruited white cells, and macrophages infiltrate the damaged layers. Proteolytic enzymes are released, fluid volume increases, and the inflammatory zone establishes a boundary layer between viable tissue and necrotic tissue.

Post-Tx Cooling and Re-Epithelization

Thermal relaxation in an actual lower eyelid procedure dropped to below baseline and recovered slowly over three days. The post-treatment cooling we observed is possibly caused by thermal convection associated with evaporation of extracellular water in dermal layers. Since removal of the stratum corneum and epidermis as a result of laser resurfacing eliminates the body's primary vapor barrier [33], it appears that significant post-treatment evaporative cooling will lower surface temperatures at the treatment site. The time course of return to baseline temperature corresponds with the time course of re-epithelization. That is, evaporative cooling subsides with the growth of the epithelium and the closing of the surface vapor barrier.

Erythema/Edema Subside

We have determined that erythema resolves rapidly. Many patients could mask the erythema with makeup within a few days and 50% of the patients had no erythema at two weeks. By 4 weeks 80% had recovered and by two months, 97%. Clinically visible tissue edema lasted 4–6 weeks. This tended to hide residual wrinkles so that patients "looked better" around 1–2 months post-Tx than they did at three months.

The causes of post-resurfacing erythema are still uncertain. Perhaps the disappearance of erythema is related to the thickening and opacification of the epidermis as well as the gradual maturation of the new papillary dermal vasculature. There is a strong positive correlation between depth of thermal damage and the duration of erythema. The TruPulse laser causes only 50 μm of thermal damage compared to 100 μm or greater for other CO_2 lasers [e.g., 14], and erythema persists about half as long when resurfacing is done with the short pulse laser (≈ 4 weeks or less) compared to other CO_2 laser systems (≈ 6–9 weeks) [11,16,29,34,35].

Dermal Changes, Healing, and Wrinkle Reduction

The depth of thermal damage is maximum at 2–3 days, increasing by about 50% from that observed immediately in in vivo animal models [14,15,18]. Below the eschar the epidermis regenerates and damaged collagen in the upper dermal tissues is gradually replaced with newly synthesized collagen (fibrous scar tissue). Eschar slough also occurs around three days. Thomsen et al. [17,18] observed that new epithelium derives from the edges of the wound, adnexal structures, and deeper uninjured dermal layers.

Dermal fibrous scar formation, a secondary response to thermal injury, is obvious by day 5 after epidermal regeneration [18]. The new growth is restricted to a uniform layer of scar tissue in the papillary dermis. The uniform thickness of this layer is likely related to the uniformity of the thermal injury. One would predict that Mesa Mode would produce a more uniform layer of new collagen than gaussian beams [8]. This subdermal scar tissue consists of a layer of collagen bands oriented parallel to the skin surface that produce a smooth contracted skin contour. The layer of new collagen continues to mature, and there follows a continuous, long term contraction over several weeks or months [18], similar to the time course of wrinkle reduction (Figure 11).

From three to nine months we have demonstrated a steady improvement in wrinkle reduction. Based on the observation that the two processes follow the same time course, it is likely that the final cosmetic objective of wrinkle reduction is achieved by this reorganization of the dermal protein matrix (tissue remodeling) [18,37]. Although our sample does not extend beyond nine months

our clinical impression is that wrinkles continue to improve up to one year postoperative. If this is true, then the data shown for wrinkle improvement in Figure 11A may not represent *final* wrinkle improvement, which could be even greater.

Our data support the hypothesis of a trend in wrinkle reduction being slightly more effective in older patients. However, it may be that a straight line is not the best fit for the data (Fig. 11C). It is possible that very young patients receive less benefit because they suffer less skin damage. However, there might also be an upper limit where aged skin does not respond well to the treatment. Unfortunately our sample over 60 years of age is too limited to identify an upper limit, if one exists.

Although our experience is limited, we would caution against resurfacing lower eyelids if the patient has had previous or concurrent standard blepharoplasty surgery. We have added this to our list of exclusion criteria to avoid the possibility of complications such as scleral show and slow healing.

Dosimetry

Several clinical investigators have reported ablation rates for resurfacing and suggest that subsequent "passes" remove a certain, constant amount of tissue [32,40]. The situation is actually more complex. First, fluence must be sufficient to exceed the threshold for ablation. Above this level the epidermal/dermal boundary appears to present a natural barrier to thermal damage, limiting ablation depth to the depth of the epidermis.

Our crater depth data suggest an ablation threshold around 3 J/cm^2 and in the same set of experiments a plume component was identified radiometrically at 3 J/cm^2. This is consistent with reports from others [7,25]. Kamat [40] identified an energy fluence of 4 J/cm^2 as the lower limit for histologic changes. Reinisch et al. [15] reported 3.7 J/cm^2 as the threshold for acute in vivo cutaneous shrinkage.

It has become obvious that the second and third pulses (passes) encounter thermally altered tissue [10,12], that is, a layer of dehydrated tissue containing hyalinized protein with an ablation threshold greater than that for intact epidermis. The threshold for tissue ablation with the second (and subsequent pulses) has not been measured. As the tissue properties change the energy coupling to the tissue varies. With the first pulse the vaporization of water consumes a large amount of the deposited energy effectively cooling the surface. After removal of the water the temperature increases and the protein is denatured.

These tissue alterations provide a barrier to further ablation. Within the range of one to four passes with the TruPulse the depth of tissue ablation and the thickness of the dermal layer of newly synthesized collagen [14,15] were not affected by number of passes. In fact, we observed the second or third pulse to actually raise the tissue surface to give a negative ablation depth. Our histology of human eyelids irradiated at 6 J/cm^2 showed no increase in ablation depth during the first four passes. Similarly, analysis of the clinical data (Fig. 11C) yielded no relation between percent wrinkle reduction and cumulative fluence within the ranges of 1–20 J/cm^2 (250–400 mJ, 1–4 passes). Apparently the appropriate tissue changes are initiated by the first pass. Passes 2–4 encounter the barrier of thermally altered tissue, no more ablation occurs, and the depth of thermal damage does not increase appreciably. Additional passes may prolong erythema, but we did not examine this relationship in our data. Acute tissue shrinkage does increase with increasing pass number [15], but the long term cosmetic consequences of this, if any, are unknown.

More aggressive dosimetry (>6 J/cm^2, >4 passes) is not recommended for eyelids but may be suitable for more robust areas of the skin. Choi et al [10] noted onset of carbonization after pulses 5–8. Perhaps this is a sign that this "barrier" is breached since from 5–20 pulses (without debridement and rehydration) we observed a linear relationship between cumulative fluence and ablation depth: the depth of the ablation crater increased by about 10 μm per pulse with 6 J/cm^2 pulses and 35 μm/pulse at 12 J/cm^2. More aggressive treatment is expected to lengthen healing time and to increase the likelihood of complications such as hypertrophic scars and dyspigmentation [7,8,19].

At a very high incident fluence of 14 J/cm^2, the shape and magnitude of the temperature profiles changed very little during the first 10 pulses. This observation implies that 14 J/cm^2 is sufficient fluence per pulse to completely vaporize the water inherent in the tissue and ablate the remaining tissue char.

Retreatment

Two patients in this study elected a retreatment option offered by the surgeon during the initial evaluation. Patient #14 was a 44-year-old female with Fitzpatrick Type 2 skin and mod-

erate wrinkles. The first treatment (cumulative fluence = 10.0 J/cm^2) resulted in wrinkle reduction of only 15%. The second treatment five months later (13.8 J/cm^2) resulted in an additional 80% reduction. Patient #21 (70 years old, T2, moderate wrinkles) was retreated at four months (First Tx: 11.0 J/cm^2, Second Tx: 10.3 J/cm^2). The first treatment resulted in a 65% reduction and the second treatment yielded an additional 80% reduction. There were no complications in either case. Re-treatment appears to be a safe and useful option.

SUMMARY

The following tissue and clinical changes are induced by laser resurfacing of human eyelids with the TruPulse Laser. The epidermis is separated from the papillary dermis and ablated with a very slight laser plume. After debridement the remaining surface consists of epidermal debris and coagulated protein from the upper dermal layers. Thermal damage extends less than 50 μm deep but increases to about 75 μm over three days. Contraction of the protein extracellular matrix causes acute tissue shrinkage of less than 5%. Inflammatory cells infiltrate the wound, thermally damaged components necrose, form an eschar, and are sloughed around three days. Reepithelization is completed by 2–7 days and erythema resolved by 2–4 weeks. A region of thermally challenged collagen is replaced with a smooth, continuous fibrous scar tissue layer in upper dermis. The collagen network continues to organize and contract over several months coincidence with a gradual increase in the reduction of rhytides.

The data support the following dosimetry for periorbital wrinkle reduction: One pass 4–6 J/cm^2 (350–500 mJ into a 3 × 3 mm spot). Within this range of fluences a second treatment after 9–12 months may be more beneficial than a second pass.

REFERENCES

1. David LM, Lask GE, Glassberg E, et al. Laser abrasion for cosmetic and medical treatment of facial actinic damage. Cutis 1989;43:583–587.
2. Fitzpatrick RE, Ruiz-Esparaza JR, Goldman MP. The depth of thermal necrosis using the CO_2 laser: A comparison of the superpulsed mode and conventional mode. J Dermatol Surg Oncol 1991;17:340–344.
3. Baker SS. Carbon dioxide laser upper lid blepharoplasty. Amer J Cosmetic Surg 1992.
4. Weinstein C. Ultrapulse carbon dioxide laser removal of periocular wrinkles in association with laser blepharoplasty. J Clin Laser Med Surg 1994;12(4):205–209.
5. Alster TS. Comparison of two high-energy, pulsed CO_2 lasers in the treatment of periorbital rhytides. Dermatol Surg 1995;22:541–545.
6. Seckel BE. Aesthetic laser surgery. Boston: Little Brown & Co., 1996.
7. Ross EV, Domanketivtz Y, Skrobal M, Anderson RR. Effects of CO_2 laser pulse duration in ablation and residual thermal damage: implications for skin resurfacing. Lasers Surg Med 1997;19:123–129.
8. Bass LE, Demallie E, Pohl D, Aston SJ. Thermal injury and tissue shrinkage in human skin in vitro after TruPulse, SilkTouch and Ultrapulse exposure: Preliminary results. SPIE 1997;2970:294–298.
9. Bell T, Harris DM, Schachter D. 100 μsec pulsed CO_2 laser resurfacing of lower eyelids: erythema and rhytid reduction. SPIE 1997;297:360–366.
10. Choi B, Barton JK, Chan EK, Thomsen SL, Welch AJ. Infrared imaging of CO_2 laser ablation: implications for laser skin resurfacing. SPIE 1998;1997:344–355.
11. Gardner ES, Reinisch L, Stricklin GP, Ellis DL. In vitro changes in non-facial human skin following CO_2 laser resurfacing: a comparison study. Lasers Surg Med 1996; 19:379–387.
12. Harris DM, Fried D, Reinisch L, Bell T, Lyver R. Thermal measurements of short duration CO_2 laser resurfacing. SPIE 1997;2970:319–326.
13. Harris DM, Bell TA, From L, Schachter D. Skin resurfacing with a very short pulsed CO_2 Laser. SPIE 1996; 2671:324–328.
14. Kuo T, Speyer MT, Reis WR, Reinisch L. Collagen thermal damage and collagen synthesis after cutaneous laser resurfacing. Lasers Surg Med 1998;23:66–71.
15. Reinisch L, Rivas M, Ossoff J, Deriso W, Sternemann J, Ossoff RH. A comparison of pulsed and continuous wave carbon dioxide laser interactions with cutaneous tissue. SPIE 1997;2970:312–318.
16. Speyer MT, Reinisch L, Cooper KA, Ries WR. Erythema after cutaneous laser resurfacing using a porcine model. Arch Otolaryngol HNS (in press).
17. Thomsen S, Baldwin B, Chi E, Ellard J, Schwartz J. Histopathology of laser skin resurfacing. SPIE 1997;2970: 287–293.
18. Thomsen S, Ellard J, Schwartz J, Nolan K. Chronology of healing events in pulsed CO_2 laser skin resurfacing in fuzzy rats. SPIE 1998;3245:337–343.
19. Weisberg NK, Kuo T, Torkian B, Reinisch L, Ellis DL. Optimizing fluence and debridement effects on cutaneous resurfacing CO_2 laser surgery. Ach Derm (in press).
20. Welch AJ, Chan E, Barton J, Choi B, Thomsen S. Infrared imaging of CO_2 laser resurfacing. Proc SPIE 1997; 2970:305–311.
21. Fried, Seka W, Glena RE, Featherstone JDB. The thermal response of dental hard tissues to (9–11 μm) CO_2 laser irradiation. Optical Engineering 1996;35(7):1976–1984,.
22. Fried, Visuri SR, Featherstone JDB, Seka W, Glena RE, Walsh JT, McCormack SM, Wigdor HA. Infrared radiometry of dental enamel during Er:YAG and Er:YSGG laser irradiation. J Biomedical Optics 1996;1(4):455–465.
23. Fried, Seka WD, Featherstone JDB, Glena RE. Multiple

pulse irradiation of dental hard tissues at CO_2 laser wavelengths. SPIE 1995;2394:41–50.
24. Fried, Borzillary SF, McCormack SM, Glena RE, Featherstone JDB, Seka W. The thermal effects on CO_2 laser irradiated dental enamel at 9.3, 9.6, 10.3, and 10.6 μm. Lasers in surgery: advanced characterization, therapeutics, and systems IV, SPIE 1994;2128:319–328.
25. Walsh JT, Flotte TJ, Anderson RR, Deutsch RF. Pulsed CO_2 laser tissue ablation: effect of tissue type and pulse duration on thermal damage. Lasers Surg Med 1988;8: 108–118.
26. Green HW, Domankevitz Y, Nishioka N. Pulsed carbon dioxide laser ablation of burned skin: In vitro and in vivo analysis. Lasers Surg Med 1990;10:476–484.
27. Zweig AD, Meierhofer B, Müller OM, et al. Lateral thermal damage along pulsed laser incisions. Lasers Surg Med 1990;10:262–274.
28. McKenzie AL. A three-zone model of soft tissue damage by a CO_2 laser. Phys Med Biol 1986;31:967–983.
29. Ostad A, Moy R. Comparison of Tru-Pulse and Silk-Touch to manual dermabraison in scar revision. Amer Soc Derm Surg, Palm Desert, CA May, 1996.
30. Klein GF, Hintner H, Schuler G, Fritsch P. Junctional blisters in acquired bullus disorders of the dermal-epidermal junction zone: role of the lamina lucida as the mechanical *locus minoris resistentiae*. Brit J Dermatol 1983;109:499–508.
31. Reid R. Physical and surgical principles governing carbon dioxide laser surgery on the skin. Dermatologic Clinics 1991;9(2):297–316.
32. Smith KJ, Skelton H, Graham JS, Hamilton TA, Hackley BE, Hurst CG. Depth of morphologic skin damage and viability after one, two, and three passes of a high-energy, short-pulse CO_2 laser (Tru-Pulse) in pig skin. J Amer Acad Dermatol 1997;37:204–210.
33. Xiao P, Imhof RE. Optothermal measurement of stratum corneum thickness and hydration depth profile. Cutaneous applications of lasers: dermatology, plastic surgery and tissue welding. SPIE 1997;2970:47–50.
34. Fitzpatrick RE. Facial resurfacing with the pulsed carbon dioxide laser: a review. Facial Plast Surg Clin North Amer 1996;4:231–240.
35. Chernoff WG, Shoenrock LD, Cramer H, Wand J. Cutaneous laser resurfacing. Int J Aesthetic Restorative Surg. 1995;3:57–68.
36. Hruza GJ. Skin resurfacing with lasers. Fitzpatrick's J Clin Dermatol. 1995;3:38–42.
37. Grevelink JM. Facial contouring using a flashscanner-enhanced carbon dioxide laser. Facial Plast Surg Clin North Amer 1996;4:241–246.
38. Ross EV, Naseef GS, Skrobal M, Grevelink JM, Anderson RR. In vivo dermal collagen shrinkage and remodeling following CO_2 laser resurfacing. Laser Surg Med 1996;18(Suppl 8):38.
39. Moy R, Bucalo B, Lee M, Wieder J, Chalet M, Ostad A. Skin resurfacing of facial rhytides and scars with the 90 microsecond short pulse CO_2 laser: Comparison to the 900 microsecond dwell time CO_2 lasers and clinical experience. (unpublished data).
40. Kamat BR, Tang SV, Arndt KA, Stern RS, Now JM, Rosen S. Low fluence CO_2 laser irradiation: selective epidermal damage to human skin. J Invest Dermatol 1985; 85:274–278.